The mediating role of mammographic density in the protective effect of early-life adiposity on breast cancer risk: a multivariable Mendelian randomization study

Marina Vabistsevits[1, 2] *, George Davey Smith[1, 2], Tom G. Richardson[1, 2], Rebecca C. Richmond[1, 2], Weiva Sieh[3,4], Joseph H. Rothstein[3,4], Laurel A. Habel[5], Stacey E. Alexeeff[5], Bethan Lloyd-Lewis[6] & Eleanor Sanderson[1, 2]

1 - University of Bristol, MRC Integrative Epidemiology Unit, Bristol, United Kingdom,
2 - University of Bristol, Population Health Sciences, Bristol, United Kingdom,
3 - Icahn School of Medicine at Mount Sinai, Department of Genetics and Genomic Sciences, Department of Population Health Science and Policy, New York, NY, United States,
4 - University of Texas MD Anderson Cancer Center, Department of Epidemiology, Houston, TX, United States,
5 - Kaiser Permanente Northern California, Division of Research, Oakland, CA, United States,
6 - University of Bristol, School of Cellular and Molecular Medicine, Bristol, United Kingdom

** Corresponding author: Marina Vabistsevits, MRC Integrative Epidemiology Unit, Population Health Sciences, Bristol Medical School, University of Bristol, UK. E-mail: marina.vabistsevits@bristol.ac.uk*

Abstract

Observational studies suggest that mammographic density (MD) may have a role in the unexplained protective effect of childhood adiposity on breast cancer risk. Here, we investigated a complex and interlinked relationship between puberty onset, adiposity, MD, and their effects on breast cancer using Mendelian randomization (MR).

We estimated the effects of childhood and adulthood adiposity, and age at menarche on MD phenotypes (dense area (DA), non-dense area (NDA), percent density (PD)) using MR and multivariable MR (MVMR), allowing us to disentangle their total and direct effects. Next, we examined the effect of MD on breast cancer risk, including risk of molecular subtypes, and accounting for genetic pleiotropy. Finally, we used MVMR to evaluate whether the protective effect of childhood adiposity on breast cancer was mediated by MD.

Childhood adiposity had a strong inverse effect on mammographic DA, while adulthood adiposity increased NDA. Later menarche had an effect of increasing DA and PD, but when accounting for childhood adiposity, this effect attenuated to the null. DA and PD had a risk-increasing effect on breast cancer across all subtypes. The MD single-nucleotide polymorphism (SNP) estimates were extremely heterogeneous, and examination of the SNPs suggested different mechanisms may be linking MD and breast cancer. Finally, MR mediation analysis estimated that 56% (95% CIs [32% - 79%]) of the childhood adiposity effect on breast cancer risk was mediated via DA.

In this work, we sought to disentangle the relationship between factors affecting MD and breast cancer. We showed that higher childhood adiposity decreases mammographic DA, which subsequently leads to reduced breast cancer risk. Understanding this mechanism is of great importance for identifying potential targets of intervention, since advocating weight gain in childhood would not be recommended.

Introduction

Breast cancer is the most common cancer in women worldwide [1]. Incidence rates continue to rise globally [2], and thus there is an urgent need to identify new and modifiable breast cancer risk factors. It is also critical to investigate the links between protective traits and breast cancer as those may reveal new mechanisms for targeted intervention. Observational and Mendelian randomization (MR) studies have shown that adiposity in childhood may reduce the risk of breast cancer in later life [3]–[7], and that this effect is direct and independent of adult body size. MR is an approach to causal inference that uses genetic variants as instrumental variables (IVs) to infer whether a modifiable health exposure influences a disease outcome [8] [9]. In previous work [10], we used an MR framework to investigate the biological mechanism underlying the protective effect of childhood adiposity by reviewing several potential mediators, including hormonal, reproductive, and glycaemic traits. However, none of the investigated mediators sufficiently explained the protective effect of childhood adiposity on breast cancer risk. A mediator that has not yet been thoroughly investigated is mammographic density (MD), an established risk factor for breast cancer [11], [12].

MD refers to the radiological appearance of fibroglandular vs adipose tissue in the breast and is frequently quantified in three phenotypes: dense area (fibroglandular tissue, DA), non-dense area (adipose tissue, NDA) and percent density (dense area as a proportion of total breast size, PD). DA and PD are associated with an increased risk of breast cancer, whereas NDA is independently associated with a decreased risk [13]. A high DA and PD elevate breast cancer risk as tumours are more likely to arise in fibrous tissue, as well as being more difficult to detect in dense areas on a mammography exam [14]. MD is highly heritable [15] and the risk of developing cancer is 4-6 fold higher in women with extremely dense vs fatty breasts [14], but MD appears to be similarly associated with all breast cancer molecular subtypes [16], [17]. Although the association between MD and breast cancer is well-established, the molecular and cellular events that lead to the development of MD and why it is associated with increased cancer risk are not well understood [18].

Growing evidence points to associations between childhood adiposity, puberty onset, and adult mammographic density (reviewed in [18]). Puberty is a critical time for breast development, during which the breast epithelial and stromal compartments undergo extensive growth and tissue remodelling [19]. Later age at menarche has been shown to positively associate with higher MD [20], [21], despite being associated with a decreased risk of breast cancer [22] [23]. Adiposity at different developmental stages also affects MD, as increased body size in adolescence is associated with a higher abundance of adipose non-dense tissue and lower dense area and percent density in adulthood [18], [20], [24], [25]. Childhood adiposity also has a well-established effect of decreasing age at menarche [26], which in turn leads to higher adult adiposity [27]. Taken together, these traits appear to have a complex and interlinked relationship that impacts breast development and growth, and ultimately breast cancer risk. Several recent observational studies have suggested that childhood adiposity may confer long-term protection against breast cancer via its effect on mammographic breast density [28]–[31]. The effect of MD on breast cancer has also been analysed using different MR methods [10], [32], [33]. While the overall picture reported from these studies supported observationally known associations, there were some differences depending on the MR method employed suggesting sensitivity to the underlying assumptions.

Here, we explore the mediating role of mammographic density in the protective effect of high childhood adiposity on breast cancer risk, using data from genome-wide association study (GWAS) studies of childhood body size, adult body size, age at menarche, mammographic density, and breast cancer within a Mendelian randomization framework.

Results

Study overview

In this study, we aimed to investigate the mediating role of mammographic density in the protective effect of childhood adiposity on breast cancer risk. Figure 1 presents a flow diagram of the relationships between the investigated traits. The summary of all analyses conducted is presented in Table 1. First, we examined the effect of body size (childhood and adulthood) on mammographic density (dense area, non-dense area, percent density) using univariable MR and multivariable MR (MVMR) [25]. We then reviewed the role of age at menarche in the childhood body size effect on MD phenotypes. Next, using data from the Breast Cancer Association Consortium (BCAC) [35][36] (Supplementary Table S1), we assessed the effect of MD phenotypes on breast cancer risk. We further investigated pleiotropy among the genetic instruments for the MD phenotypes using a variety of advanced sensitivity analysis methods [37]–[39], PheWAS [40], and pathway analysis, to dissect their heterogeneous effect and improve the understanding of the MD effect on breast cancer. Finally, we performed MVMR of childhood body size and MD phenotypes with breast cancer risk and mediation analysis to assess the direct and indirect effects of both traits and evaluate the role of MD in the poorly understood protective effect of childhood body size on breast cancer.

This study is reported as per the guidelines for strengthening the reporting of Mendelian randomization studies (STROBE-MR) [41] [42].

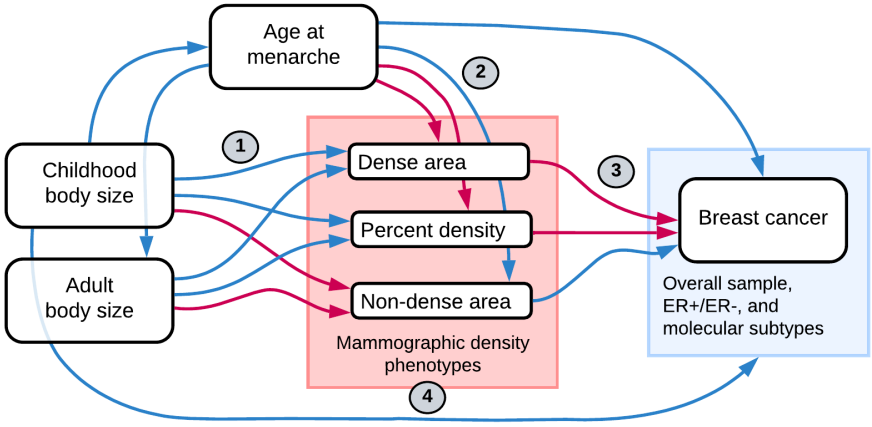

Figure 1. Flow diagram of relationships between traits investigated in this study. Blue arrows indicate a negative (decreasing / protective) effect and pink arrows show a positive (increasing / causal) effect relationship, as previously reported in the literature. The numbers signpost the analysis sections, which are mentioned throughout the text and correspond to the numbers in the analysis summary in Table 1.

Table 1. Summary of analyses conducted. The table is split into sections (#) for convenient reference throughout the text. Mammographic density (MD) is available as three phenotypes: Dense area (DA), non-dense area (NDA), and percent density (PD); data source: Sieh *et al* (2020) [32]. Breast cancer outcomes include data from BCAC 2017 and 2020 (overall samples, ER+/ER- samples and five molecular subtypes: Luminal A, Luminal B1, Luminal B2, HER2-enriched, and triple-negative; summarised in Supplementary Table S1; data sources: [35][36]). Childhood/adult size body and age at menarche data are UK Biobank phenotypes from Richardson *et al* (2020) [5]. In the table, when several exposures/outcomes are listed (e.g. MD phenotypes or cancer subtypes), this indicates that MR analysis was done separately for each, unless they are two exposures in MVMR. MR – Mendelian randomization, MVMR – multivariable MR, BCAC – Breast Cancer Association Consortium

#	Analysis type	Exposure trait(s) represented as genetic instruments	Phenotypic outcome traits(s) *(when applicable)*	Results available in
1	MR	Childhood body size	Mammographic density (DA, NDA, PD)	Figure 2a, Table S3
	MR	Adult body size	Mammographic density (DA, NDA, PD)	
	MVMR	Childhood body size, Adult body size	Mammographic density (DA, NDA, PD)	Figure 2b, Table S5
2	MR	Age at menarche	Mammographic density (DA, NDA, PD)	Figure 2a, Table S7
	MVMR	Childhood body size, age at menarche	Mammographic density (DA, NDA, PD)	Figure 2c Table S9
3	MR	Dense area (DA)	Breast cancer (overall and subtypes)	Figure 3a, Table S11
	MR	Non-dense area (NDA)	Breast cancer (overall and subtypes)	
	MR	Percent density (PD)	Breast cancer (overall and subtypes)	
4	MVMR	Childhood body size, Dense area (DA)	Breast cancer (overall and subtypes)	Figure 3b, Table S13
	MVMR	Childhood body size, Non-dense area (NDA)	Breast cancer (overall and subtypes)	
	MVMR	Childhood body size, Percent density (PD)	Breast cancer (overall and subtypes)	
5	MR-PRESSO	Mammographic density (DA, NDA, PD)	Breast cancer overall sample	Figures 4a, S4a, S6a Table S16
	Radial-MR	Mammographic density (DA, NDA, PD)	Breast cancer overall sample	Figures 4b, S4b, S6b Table S17
	MR-Clust	Mammographic density (DA, NDA, PD)	Breast cancer overall sample	Figures 4c-d, S4c-d, S6c-d Table S18
6	PheWAS	Mammographic density (DA, NDA, PD)	N/A	Figure 5, S5, S7 Tables S19-S21
7	Pathway analysis	Mammographic density (DA, NDA, PD)	N/A	Tables S22-27
8	Mediation analysis	Childhood body size, Dense area (DA) (as a mediator)	Breast cancer overall sample	Supplementary Note 2

The effect of childhood and adult body size on mammographic density

We used univariable MR to evaluate the total effect of childhood and adult body sizes on each MD phenotype (analysis #1 in Table 1 and Figure 1). This analysis was performed using MD GWAS data unadjusted for adult BMI to avoid double adjustment for BMI in MVMR analyses; the details of this and subsequent analyses using MD GWAS data adjusted for adult BMI (i.e. the data from the original publication of MD GWAS [32]) are available in Supplementary Note 1. We found evidence that larger body size, both during childhood and as an adult, reduces dense area and percent density, but increases non-dense area (Figure 2a, Supplementary Table S3). The estimates from these analyses reflect the standard deviation (SD) change in MD phenotype for each change in childhood and adult body size category. We also performed multivariable MR including both childhood and adult body size to estimate the direct effects of body size at each age on MD conditional on the other age (Figure 2b, Supplementary Table S5). In this analysis, a direct effect was demonstrated for both traits,

however, larger childhood body size had a stronger effect on decreasing dense area, while larger adult body size had a stronger effect on increasing non-dense area (adipose tissue area of the breast). The direct effect on percent density was greater from adult body size, but its magnitude was considerably reduced in MVMR for both measures.

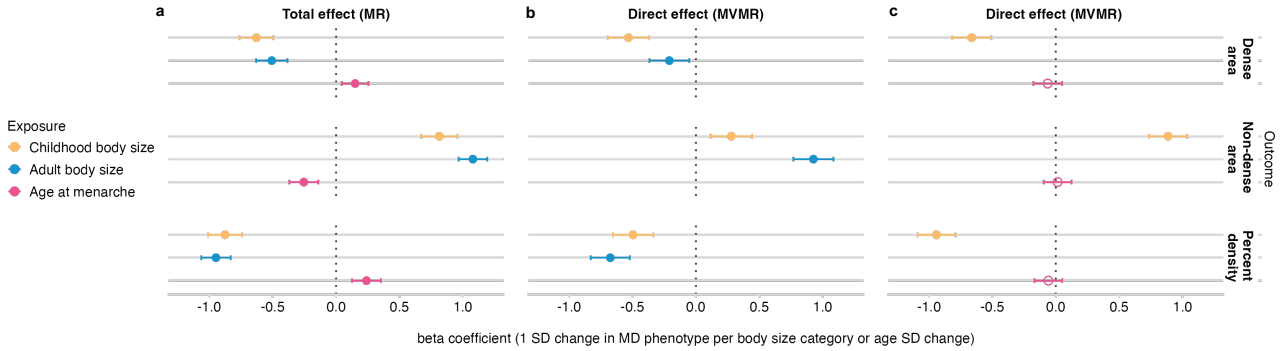

Figure 2. Univariable MR (total effect) and multivariable MR (direct effect) results of childhood body size, adult body size, and age at menarche effect on MD phenotypes (dense area, non-dense area, percent density) (unadjusted for BMI at GWAS level). (a) Total effect of each exposure on MD outcomes. (b) Direct effects of childhood and adult body sizes on MD outcomes. (c) Direct effects of childhood body size and age at menarche on MD outcomes. The effect is measured as the standard deviation (SD) change in MD phenotype per body size category or age at menarche SD change. Bars indicate 95% confidence intervals around the point estimates from MR/MVMR IVW analyses. The empty circle data points highlight the results where confidence intervals overlap the null.

The effect of childhood body size and age at menarche on mammographic density

In this MR analysis, we sought to analyse childhood body size and age at menarche together to evaluate their total and direct effects on MD phenotypes (analysis #2 in Table 1 and Figure 1). In univariable MR (Figure 2a, Supplementary Table S7), childhood body size and age at menarche had strong opposing effects on MD (DA and PD), which is in agreement with published studies [20] [21], [25]. In MVMR (Figure 2c, Supplementary Table S9) the direct effect of body size conditional on age at menarche is similar to the total effect, while the effect of age at menarche is attenuated to overlap the null. Adiposity in childhood reduces MD and lowers the age at menarche (as shown in [10]), while younger age at menarche has a negative effect on MD (i.e. the inverse of higher age at menarche increasing MD in Figure 2a). The attenuation of age at menarche effect can be explained in the following way: (1) the direct effect of childhood adiposity is maintained in MVMR when accounting for age at menarche, suggesting that adiposity affects MD independently of starting puberty earlier, (2) the menarche effect in univariable results is not present in MVMR results suggesting that it is largely due to unaccounted increased childhood adiposity (and its effect on the initiation of puberty). Collectively, our results show that the density-decreasing effect of larger childhood body size is not acting via lowering the age at menarche, and that childhood body size and age at menarche may have entirely different mechanisms linking them to breast cancer.

The effect of mammographic density on breast cancer

Next, we evaluated the effect of BMI-unadjusted MD phenotypes on breast cancer (analysis #3 in Table 1 and Figure 1) using IVW MR estimation. The total effect of MD phenotypes on breast cancer subtypes is presented in Figure 3a (Supplementary Table S11). Overall, we found a consistent trend in the direction of effect across all breast cancer subtypes for each MD exposure trait: dense area and percent density increased the risk, while non-dense area decreased the risk, which is in line with the observational data. Despite being consistent, many estimates were imprecise, however, there was stronger evidence for a positive effect of dense area on overall breast cancer, ER+ breast cancer, and several subtypes. The individual SNP-specific effects within all MD phenotypes' total estimates were heterogeneous (detailed below under **Sensitivity analysis**), and therefore, in the

Dissecting the mammographic density effect using robust MR methods section we explore those effects using various sensitivity and outlier detection methods. The direct effects from the MVMR analysis in Figure 3b are discussed in a later section.

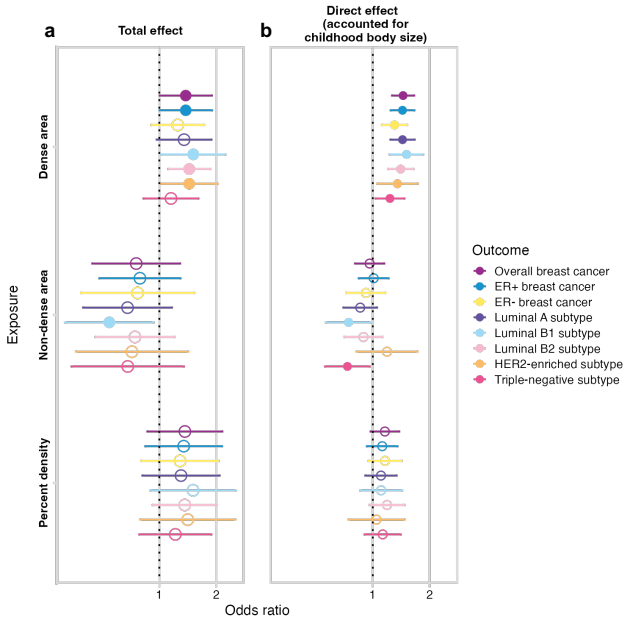

Figure 3. (a) The total (univariable MR) and (b) direct (accounted for childhood body size, MVMR) effect of MD phenotypes (unadjusted for BMI) on breast cancer (overall sample from BCAC 2017 and subtype samples). The plots show the odds of breast cancer per SD increment in MD phenotype. Bars indicate 95% confidence intervals around the point estimates from IVW and IVW-MVMR analyses. The empty circle data points highlight the results where confidence intervals overlap the null.

Sensitivity analysis

To investigate potential violations of the MR assumptions and validate the robustness of the two-sample IVW MR results, we performed additional MR analyses using MR-Egger [43] and weighted median [44] approaches, both of which provide sensitivity analyses that are more robust to particular forms of horizontal pleiotropy. The Egger intercept was used to explore the potential for the presence of directional horizontal pleiotropy, and Cochran's Q statistic [45] was calculated to quantify the extent of heterogeneity among SNPs, which is indicative of potential pleiotropy. For MVMR we tested instrument strength, using a conditional F-statistic [46] and examined heterogeneity using an adapted version of the Q-statistic (Q_A).

The estimated total effects of childhood and adult body size measures on MD phenotypes were consistent across MR sensitivity analyses with Egger intercept 0.01 or lower. The F-statistics were > 10 and Q-statistics did not indicate excessive heterogeneity (Supplementary Table S4). In MVMR, the conditional F-statistics were also above 10, indicating that weak instrument bias is unlikely to be present [46]. The presence of directional pleiotropy was assessed by estimating Q_A statistics, which also were not notably large (Supplementary Table S6).

The direction of effect was consistent among the MR methods when assessing age at menarche effect on MD phenotypes, but there was less robust evidence of effect in the weighted median result. The F-statistic for age at menarche was above 10; the Egger intercept was substantially close to zero (~0.002), indicating little evidence of directional pleiotropy [47]. The Cochran's Q value was large with p-values <2e-10, indicating high heterogeneity (Supplementary Table S8). In MVMR of age at menarche and childhood body size, the F-statistics were above 10, and Q_A was similar to the Q value in the univariable analysis (Supplementary Table S10).

In the main IVW analysis of MD phenotypes effect on breast cancer outcomes, the evidence was present only in selected exposure-outcome pairs, as described in the previous section. Applying sensitivity methods to those results showed some inconsistency, with MR-Egger producing imprecise results. The weighted median approach, which relies on at least 50% of the variants' total weight being from valid instruments [44], provided evidence for an effect in substantially more analyses than IVW, which relies on 100% of variants being valid instruments, indicating that some variants may be outliers (Supplementary Table S11). The Egger intercept in the analyses of non-dense area and percent density with subtype outcomes suggested likely presence of horizontal pleiotropy. The intercept in analyses of dense area, where evidence of effect was present in IVW, was smaller, indicating that dense area phenotype is less subject to pleiotropy. The MD phenotypes' instrument strength was good (F-statistics > 10) suggesting that weak instruments are unlikely to be a source of serious bias in the univariable analysis. Steiger filtering did not indicate that MD phenotypes' instruments explained more variance (R^2) in breast cancer rather than in MD phenotypes, and therefore, were not excluded from the analysis. Interestingly, we identified substantial heterogeneity for all MD phenotypes, suggested by very high Q-values with small p-values. High heterogeneity may be indicative of one or more variant outliers in the analysis, which was explored with additional sensitivity in the next section. The sensitivity analysis details are available in Supplementary Table S12.

Dissecting the mammographic density effect using robust MR methods

To explore the high heterogeneity in the genetic instruments for the MD phenotypes, we applied several methods that aim to dissect heterogeneity and assess potential horizontal pleiotropy through outlier detection (analysis #5 in Table 1). In this investigation, we focused only on the overall breast cancer sample outcome.

We used MR-PRESSO [37] and Radial-MR [39] (see **Methods**) to identify the variant outliers (Supplementary Tables S16-17). For dense area, both methods determined the same set of SNPs as outliers (Figures 4a and 4b). The outlier-corrected total IVW estimates are presented below the single SNP forest plots (outlier SNPs are highlighted), alongside the results of other MR methods. With outliers removed, the point estimate (OR 1.40 [1.26: 1.56]) is similar to the original IVW result (OR 1.38 [1.002: 1.90]), but the confidence intervals are more precise. Consequently, the outlier-corrected IVW estimates of dense area had stronger evidence of effect on breast cancer, and were similar to weighted median method results (OR 1.25 [1.12: 1.39]).

Next, we used MR-Clust [38] to investigate the presence of clustered heterogeneity among the genetic variants. MR-Clust groups genetic variants into clusters with similar estimates for the causal effect of the exposure on the outcome (i.e. based on their direction, magnitude, and precision). A cluster may represent a distinct pathway through which exposure is related to the outcome, and investigating heterogeneous estimates in this way may reveal additional information about the exposure-outcome relationship (see **Methods** for further details). MR-Clust detected three distinct clusters ('cluster_1', 'cluster_2', 'cluster_3'), a 'null' cluster, and two 'junk' SNPs that were not assigned to any of the clusters (Figure 4c, Supplementary Table S18). We see that the heterogeneity outliers flagged by MR-PRESSO and Radial-MR (Figures 4a and 4b) represent separate clusters in MR-Clust (Figure 4d). 'Cluster_2' (blue) is equivalent to the outlier-corrected estimate from those earlier analyses and the variants in this cluster are positively associated with an increase in both dense area and breast cancer risk. 'Cluster_3' (orange) and a positive 'junk' SNP are associated with breast cancer to a higher magnitude (Figure 4c) and therefore form a separate cluster. Interestingly, the SNPs in 'cluster_1' are protective of breast cancer despite being associated with increased density. It is important to note that both the inverse association ('cluster_1') and the same direction but higher magnitude association ('cluster_3') clusters add to the overall heterogeneity of the total estimate.

The results for non-dense area and percent density phenotypes are presented in Supplementary Figures S4 and S6. We similarly found outliers and clusters in those traits' instruments. However, due to the lower number of instruments available for these traits, the results from MR-PRESSO and Radial-MR should not be overinterpreted. The outlier-corrected IVW estimates (non-dense area –

OR 0.75 [0.65: 0.86] and percent density – OR 1.29 [1.16: 1.44]) were similar to the weighted median method results (OR 0.74 [0.63: 0.87] and OR 1.32 [1.14: 1.53], respectively) (Supplementary Tables S16 and S17). In MR-Clust, for non-dense area and percent density, there were also variants that associated with breast cancer in the opposite direction to the overall and expected effect from the exposure (e.g. negatively associated with breast cancer risk but positively associated with a factor causal for breast cancer, or vice versa) – two 'negative effect' outliers for percent density and one 'positive effect' outlier for non-dense area).

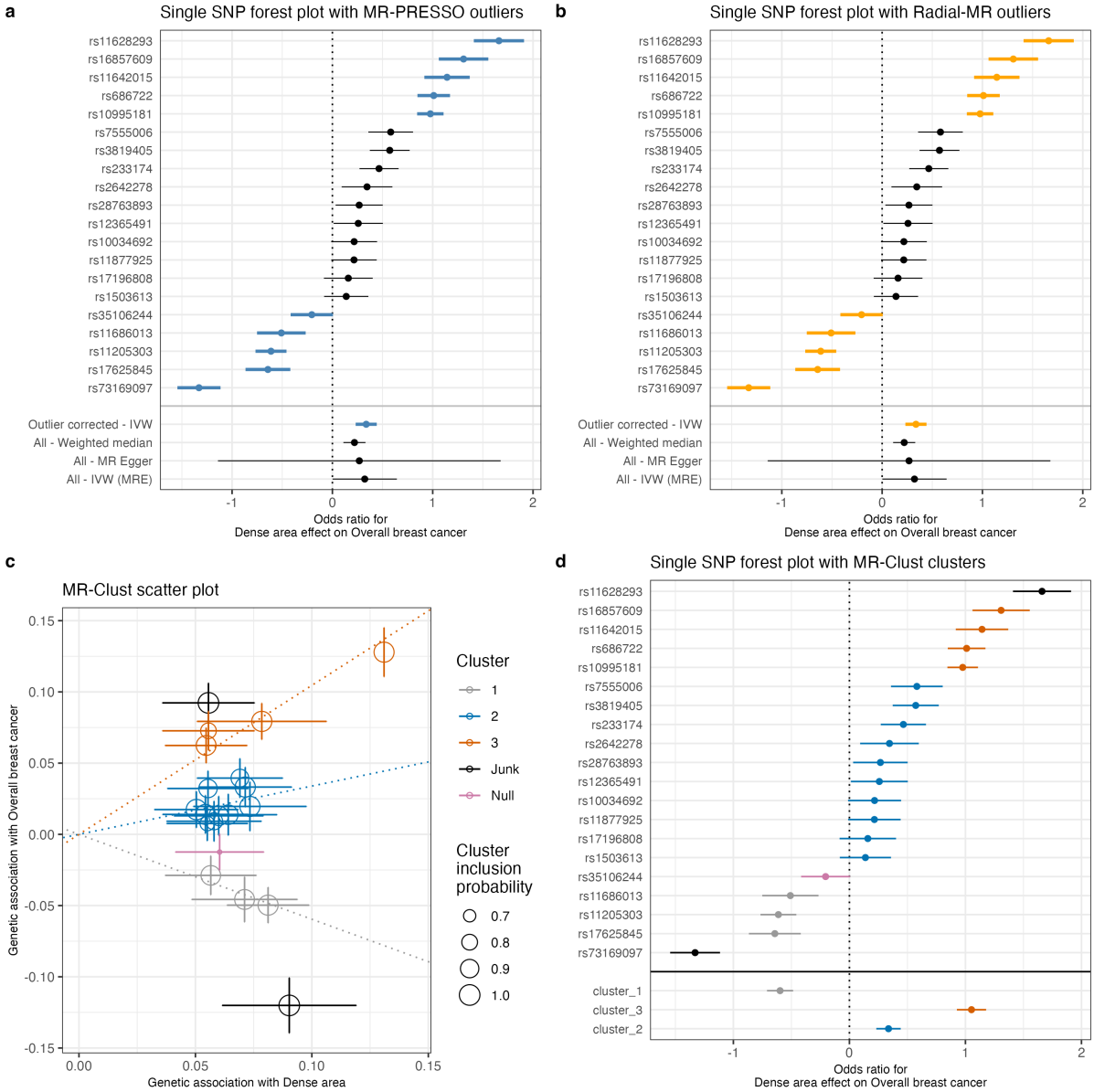

Figure 4. Exploring the heterogeneity of genetic instruments of dense area phenotype on overall breast cancer (BCAC 2017). (a) Single SNP forest plot (Wald Ratio estimates), with SNPs identified as outliers by MR-PRESSO marked in blue. The outlier corrected estimate is presented along with the standard MR methods estimates. **(b)** Single SNP forest plot with SNPs identified as outliers by Radial-MR marked in yellow. The outlier corrected estimate is presented along with the standard MR methods estimates. **(c)** MR-Clust scatter plot showing genetic association with dense area and breast cancer per SD change in dense area. Each genetic variant is represented by a point. Error bars are 95% confidence intervals of the Wald Ratio for each variant. Colours represent the clusters, and dotted lines represent the cluster means, the point size denotes cluster inclusion probability. The "null" cluster, coloured pink, relates to variants with null effect, whilst the black "junk" cluster are variants that were not assigned to any cluster. The error bars denote the standard error estimates of the Wald Ratio for each instrumental variable. **(d)** Single SNP forest plot with SNPs coloured by the cluster membership assigned by MR-Clust (using the same colours as in the scatter plot). The IVW MR estimates for each cluster are presented below single SNP estimates. IVW – inverse-variance weighted; MRE – multiplicative random effects

PheWAS

We carried out a phenome-wide association study (PheWAS) analysis [40] on the genetic instruments for the MD phenotypes to examine their associations with other traits (analysis #6 in Table 1). We aimed to review the differences between associations by clusters identified with MR-Clust and evaluate whether outlier SNPs may be strongly associated with other phenotypes, which may explain the horizontal pleiotropic effect and hint at alternative causal pathways for those outliers.

The PheWAS results for the dense area phenotype are plotted in Figure 5. The SNPs that were identified as outliers in previous analyses and that formed distinct clusters from the main effect clusters, have a higher number of associations with other traits, highlighting their pleiotropic effect. In the plot, we use the diamond shape to indicate dense area SNPs that associate strongly (p-value < 5e-08) with breast cancer. Those SNPs correspond to 'cluster_3', 'cluster_1', and 'junk' cluster SNPs in the MR-Clust results, here similarly flagging their association with breast cancer risk, which may be happening via a different pathway other than through dense area.

PheWAS plots for non-dense area and percent density are available in Supplementary Figures S5 and S7. For those phenotypes, similarly, we found associations with breast cancer for the outlier SNPs. All found associations are available in Supplementary Tables S19-21.

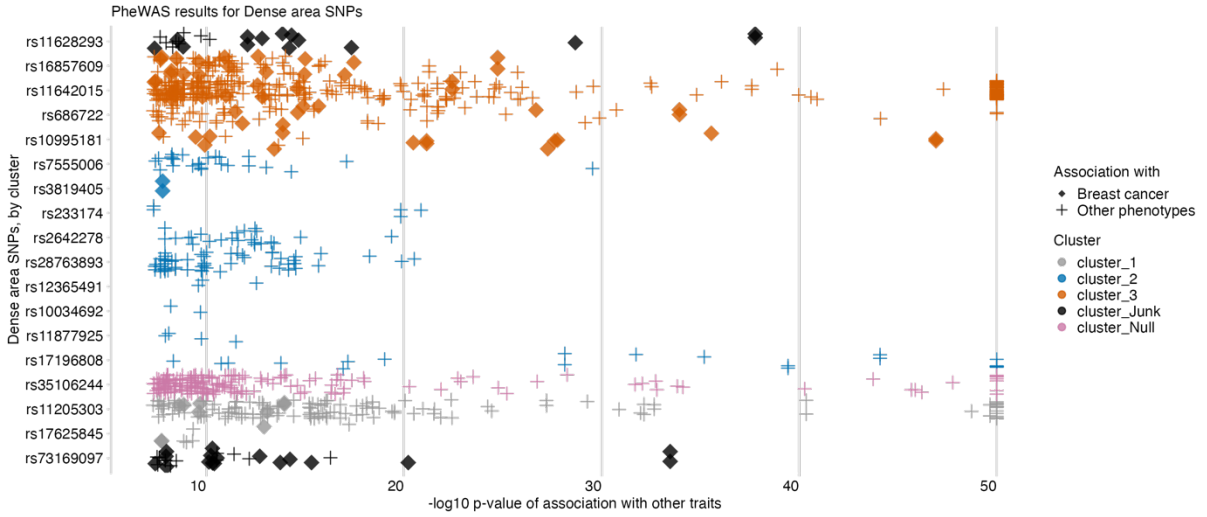

Figure 5. PheWAS results for dense area phenotype genetic variants, ordered by SNP effect and cluster membership (from MR-Clust). The data points are other traits associated with dense area SNPs (y-axis) at p-value <5e-08 (x-axis, -log10 scale, capped at value 50). The colour shows the cluster membership, in the same palette and order as in Figures 4c/4d. Data points represented by solid 'diamond' shapes are breast cancer outcomes; 'plus' shapes are all other traits.

Gene and pathway overview

To gain some biological context for the identified outlier SNPs and distinct clusters, we mapped instrument SNPs to genes (Supplementary Tables S22-24; see gene-labelled forest plots in Supplementary Figure 8) and identified pathways that those genes are involved in (analysis #7 in Table 1). Performing a formal gene-set enrichment analysis was not possible here due to the limited number of SNPs available for each phenotype/cluster. Therefore, instead, we created a simple overview of pathway sets that came up for genes in positive and negative effect clusters (Supplementary Table S25-27, Supplementary Figure 9).

For dense area, we found a number of unique pathways that only appeared in genes/SNPs with a negative effect. Among those genes, most were described in the functional analyses of previously published MD GWAS [48], [49], [32], such as *MKL1/MRTFA* (rs73169097 – negative 'null' cluster SNP) and *MTMR11* (rs11205303), both of which have dense phenotype-increasing effect but are protective against breast cancer. The potential tumour-inhibiting and tumour-promoting role of MKL1

was previously acknowledged in [48]. *MTMR11* is negatively associated with both dense area and percent density (but as a result of LD clumping it is an instrument only for dense area). It appears to be involved in phosphoinositides/phosphatidylinositol metabolism pathways, which are also implicated in cancer. For percent density, the genes in negative clusters were also previously described in published functional analyses - *OTUD7B* (rs12048493) and *ZNF703* (rs4286946) [49], [50]. Interestingly, the positive outlier in non-dense area instruments is also mapped to *ZNF703* (rs75772194), which is also associated with breast size. The complete overview of cluster/genes/pathways is available in Supplementary Tables S25-27.

The direct effect of mammographic density and childhood body size on breast cancer risk

In the earlier sections, we reviewed the total effect of MD phenotypes on breast cancer risk (Figure 3a) and explored it using various sensitivity analyses. In this section, we dissect the direct effects of childhood body size and MD phenotypes on breast cancer risk using MVMR (analysis #4 in Table 1 and Figure 1). In Figure 3b (Supplementary Table S13), we see the direct effect of MD on breast cancer accounting for childhood body size, presented alongside the total effect for comparison. There is evidence of a positive direct effect from the dense area on all breast cancer subtypes. The point estimates are similar to those of the total effect, but with more precise confidence intervals. There is evidence of a negative effect from non-dense area on Luminal B1 and triple-negative subtypes, while the effects on other samples have been further attenuated towards the null. For percent density, the magnitude of effect and the uncertainty around the point estimate is reduced in MVMR analysis, with little evidence for an effect of PD on all breast cancer subtypes when accounting for childhood body size. It should be noted that IVW MVMR estimates may also be potentially biased by pleiotropy in the same way as total effect estimates in univariable MR.

From the same MVMR analysis as the results in Figure 3b, we have also estimated the direct effect of childhood body size on breast cancer accounted for MD phenotypes. Figure 6 presents the total effect of childhood body size on breast cancer (overall and subtypes) (Supplementary Table S15) along with the direct effect accounted for each MD phenotype (Supplementary Table S13). The total effect is strongly protective against all outcomes. In previous work, this protective effect was not disrupted by accounting for any hypothesised mediators [10]. In this analysis, we see that accounting for MD phenotypes attenuates the protective effect making the confidence intervals overlap the null, suggesting that MD may have a role in partially explaining it. When accounting for the dense area, the effect attenuation is seen for all outcomes except the ER- sample. For percent density, the effect on breast subtypes is attenuated but to a lesser extent, which may suggest that dense area phenotype has a stronger mediating role than percent density. For non-dense area, the effect is attenuated also on a subset of breast cancer subtypes. Interestingly, the effect on ER- subtype is the least affected, suggesting there might be some difference in how MD affects ER- breast cancer risk.

It is important to note that the number of MD instruments in this MVMR analysis was limited (Supplementary Table S2). These MVMR results are also affected by weak instrument bias, as F-statistics are low in these analyses: childhood body size and dense area (F-stat, 17 and 7, respectively) non-dense area (6 and 3), percent density (7 and 4), respectively (Supplementary Table S14).

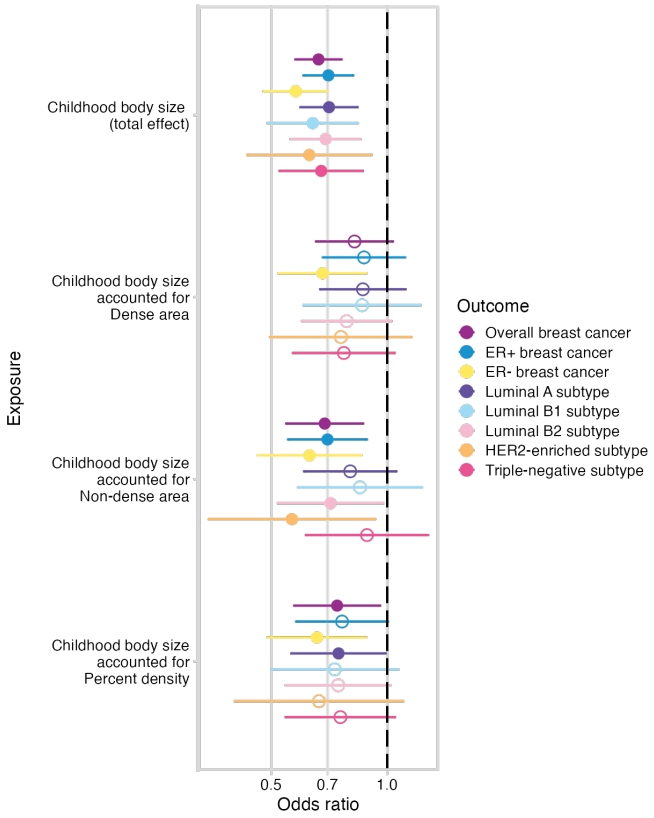

Figure 6. The total and direct effects of childhood body size (accounted for MD phenotypes – dense area, non-dense area, percent density (unadjusted for BMI at GWAS level)) on breast cancer (overall sample from BCAC 2017 and subtype samples). The plots show the odds of breast cancer per body size category change. Bars indicate 95% confidence intervals around the point estimates from IVW and IVW-MVMR analyses. The empty circle data points highlight the results where confidence intervals overlap the null.

Mediation analysis

We performed mediation analysis using MR and MVMR results to assess the role of mammographic density (specifically, dense area) in the relationship between childhood body size and breast cancer. This investigation was also done focussing only on the overall breast cancer sample (analysis #8 in Table 1).

We estimated the indirect effect via MD, using both Product and Difference methods for mediation analysis (see **Methods**). Both methods produced similar indirect point estimates in the same direction, -0.23 [95% CIs; -0.33: -0.13] and -0.22 [-0.48: 0:05], respectively. The proportion of the mediated effect via dense area using the Product method estimate was 0.56, indicating that dense area may account for 56% [32%-79%] of the childhood body size protective effect on breast cancer (see **Supplementary Note 2** for mediation analysis calculations).

Discussion

The protective effect of higher childhood adiposity on breast cancer risk has been reported in both observational and MR studies [3]–[7]. However, the mechanism behind this effect has been challenging to decipher, even after reviewing nearly 20 potential mediators [10]. A few observational studies have suggested that mammographic density may have a role in this relationship [28]–[31]. In this study, we explored the mediating role of MD in the protective effect of higher childhood adiposity on breast cancer risk using Mendelian randomization, examining the complex relationships between childhood body size, adult body size, age at menarche, mammographic density, and breast cancer risk.

Firstly, we investigated the factors that may affect MD – adiposity at different life stages and age at menarche. We found that higher childhood and higher adulthood adiposity decrease dense area and percent density, while both increase the non-dense (adipose tissue) area. In multivariable MR analysis, however, the independent direct effect of childhood adiposity was stronger for decreasing dense area, while adult adiposity was stronger for increasing non-dense area. The inverse effect of higher body size on density is likely explained by increasing breast adiposity, reducing the proportion of fibroglandular components, and increasing adipocyte differentiation of stromal cells, thus reducing collagen production [51]. As breast tissue undergoes substantial development during puberty, it is reasonable that childhood rather than adult adiposity is a more important factor for dense area. The stronger effect of adult adiposity on the non-dense area is likewise logical, as the change in MD with age is reflected in glandular tissue reduction and an increase in fat [52]. We also showed that adjustment for BMI in GWAS may lead to an unexpected and misleading result in MR analysis (Supplementary Note 1), if BMI (i.e. heritable covariate) also has a role in the studied relationship [53] [54].

The previously observed association of age at menarche with breast density [20] was replicated in our MR analysis, with later menarche increasing dense area and percent density and decreasing non-dense area. In MVMR with childhood body size, however, the effect of age at menarche on MD phenotypes was attenuated. Greater adiposity in childhood reduces dense area and percent density and lowers the age at menarche [10], while earlier menarche decreases dense area and percent density. Therefore, the attenuation of its effect in MVMR indicates that the menarche effect observed in the univariable analysis may be due in part to increased adiposity (and its effect on the initiation of puberty). Collectively, our results suggest that the density-decreasing effect of childhood body size is not acting predominantly via lowering the age at menarche.

This finding draws attention to prior MR studies showing little evidence of effect of age at menarche on breast cancer risk [10], [55]. Interestingly, in MVMR analyses when accounting for BMI, there is a shift from the neutral effect to a causal effect with earlier age at menarche increasing the risk. It is likely that the total effect of age at menarche is driven (and disguised) by childhood BMI SNPs in the age at menarche GWAS instruments, and accounting for BMI in MVMR separates the independent effects of childhood BMI and age at menarche on breast cancer risk. Taken together with our finding that MD is not affected by age at menarche when accounting for body size, this suggests that the mechanisms linking childhood adiposity and age at menarche to breast cancer could be entirely different and operate in opposite directions. Uncovering the mechanistic links in both relationships (as partly done in this work with respect to childhood body size) will identify different pathways that could be modifiable, and together could contribute a very substantial component of modifiable breast cancer risk. Another important consideration relating to mechanistic links is the distinction between mutagenesis and promoters in breast cancer causation [56], which may also contribute to the differential effects of childhood adiposity and age at menarche on breast cancer risk.

The central relationship explored in our study is that of MD and breast cancer, and whether MD helps explain the inverse association of childhood adiposity and breast cancer risk. When examining the total effect of MD phenotypes on breast cancer risk (overall and subtypes), we observed consistent trends in the direction of effects, with dense area and percent density increasing the risk and non-dense area decreasing the risk, in line with observational results [12][13]. We found evidence of a

positive effect from the dense area on breast cancer risk overall and for certain subtypes, but for other MD exposure/breast cancer outcome pairs the evidence was insufficient. The results produced by the IVW method may potentially be biased by pleiotropy, therefore the detected high levels of heterogeneity were further explored in our analysis and will be discussed below. It is also worth mentioning that our results may slightly differ from the previously published MR results using related data [10], [32], [33], which could be explained by the differences in the MR methods employed, the approach to instrument selection, and the fact that the MD GWAS was unadjusted for BMI in this study.

While the total effect of MD on breast cancer was imprecisely estimated, IVW-MVMR of MD phenotypes with childhood body size showed strong evidence of a risk-increasing direct effect from the dense area on all breast cancer subtypes, with less evidence for a negative effect of non-dense area and a lack of evidence for an effect of percent density. This highlighted the possibility that dense area is the more important risk factor for breast cancer, however in observational studies [12], percent density has been found to have a stronger association because it combines the effects of both dense area and non-dense area which have distinct genetic aetiologies [32]. The direct effect of childhood body size on breast cancer was attenuated in this MVMR analysis, suggesting a potential mediating role of mammographic density in the relationship between them. This is the first time we have observed an attenuation of the effect of childhood body size; in our previous work, where many potential mediations were assessed, the body size effect remained unaffected [10]. Interestingly, this attenuation of effect was not present in analyses of ER-negative breast cancer, suggesting that there might be some differences in how MD affects this disease subtype. We considered including adult body size and age at menarche as covariates in MVMR, however, we opted not to pursue this analysis due to concerns about the statistical power.

In addition to the effect changes observed in MVMR, we conducted a formal mediation analysis with the dense area phenotype. Both mediation methods we applied produced very similar indirect effect estimates (-0.23 and -0.22, Product and Difference methods, respectively). Such agreement of estimates was not the case for other mediators we reviewed in our previous work [10]. The confidence intervals around these estimates were more precise for the Product method -0.23 [-0.33: -0.13]). The calculated proportion mediated via dense area suggested that 56% [32%-79%] of childhood adiposity's protective effect could be due to it decreasing the dense area in childhood, which leads to reduced breast cancer risk in adulthood.

The above finding is promising, however, the relationship of MD phenotypes with breast cancer is complex and, as shown in our sensitivity analyses, the genetic variants used in the analysis have heterogeneous estimates and are potentially highly pleiotropic. We thoroughly evaluated the dense area, non-dense area, and percent density genetic instruments using several robust MR outlier detection methods and an MR clustering method, MR-Clust, to decompose heterogeneity in the results. For dense area and percent density, we found a set of outlier SNPs that together formed 'negative effect' clusters, which mapped to genes that were associated with higher dense area/percent density, but a decreased cancer risk. This has been previously reported for the same identified genes, e.g. *MLK1* in [48] and *MTMR11* in [49]. Similarly, for the non-dense area, we found one SNP with the opposite effect on breast cancer to the overall effect direction. The PheWAS analysis highlighted the fact that outlier SNPs, which also form separate clusters of MD effect on breast cancer, were highly pleiotropic, with the majority also associated with breast cancer. Several methods for outlier correction showed that removing those SNPs results in stronger and more consistent effects of MD phenotypes on breast cancer risk.

The discovery of multiple MD variants that are also breast cancer susceptibility loci, highlights their shared genetic component and the critical role MD plays as an intermediate phenotype for the disease. The inconsistency in the direction of associations between some MD-associated SNPs and breast cancer risk is perplexing, and is the reason for the observed heterogeneity in MR estimates. One potential explanation for discrepancies in these variants may be that multiple alternative pathways are involved, and are acting across different life stages, which differentially affect breast development and the risk of breast cancer. There is also a strong possibility that not all contributors to MD influence breast cancer risk. Understanding, and correctly classifying the driving components

of MD (reviewed in [57]) into those that influence breast cancer risk, and using those for future studies could increase results precision and the degree of mediation detected. Motivated by a recent study that explored a similarly heterogenous effect of IGF-1 on type 2 diabetes using MR-Clust and pathway analysis [58], in our work, we attempted to characterise pathways that may be underlying the identified positive and negative effect clusters. In our case, however, due to the limited number of instruments, pathway gene-set enrichment analysis was not feasible. An extensive pathway analysis based on the MD GWAS used in our work was reported in the original publication [32].

The limitations of our study, including the precision of estimates and pathway analysis, can be attributed to the small sample size of the currently available MD GWAS data and the consequent low number of robustly associated genetic instruments. Despite using one of the largest MD GWAS cohorts to date (N=24,192) [32], the number of instruments was still relatively small (albeit higher than in earlier studies, such as [48], [59]). A summary table of all published MD GWAS studies is provided in a recent review [60]. A similarly sized MD GWAS conducted on data from the BCAC cohort (N=24,579-27,900) [61] has recently been released, but due to the unavailability of effect sizes, it is not possible to validate our findings using this resource. Once larger MD GWAS studies become available, and more SNPs with robust associations are identified, our results could be replicated. A higher number of instruments would also enable more informative clustering and pathway analyses, despite the likely maintained heterogeneity amongst individual estimates. Furthermore, the estimation of childhood body size indirect effect via MD would also likely be more precise.

It is important to highlight a few recent developments in studying the genetics of mammographic density. Firstly, the first-ever GWAS of breast tissue structure patterns (also referred to as texture features) has recently been published [62], which is an emerging independent breast cancer risk factor [63]. Texture variation can differ substantially between women, despite having the same percent density. Including this trait in the MD phenotype analyses (including MR) can produce additional insights into the development of breast cancer. Secondly, as exploring proximal molecular mediators is becoming more widespread, the analysis of MD phenotypes in the BCAC cohort [61] also included a transcriptome-wide association study (TWAS). The study revealed additional novel associations between imputed breast tissue expression level and MD phenotypes. Some of the identified genes were located in proximity to GWAS loci, suggesting the observed genotype–phenotype association for MD may be mediated through gene expression. Further, a recent transcriptomic study [64] evaluating differentially expressed pathways in breast tissue samples from obese vs normal weight adolescents, identified inflammation-related genes as among the most highly activated upstream regulators in the obese breast tissue samples.

Our study thoroughly explores the links between adiposity, puberty timing, and mammographic density, and breast cancer. The major finding of this study is that mammographic density, specifically dense area, potentially accounts for 56% of the protective effect of childhood adiposity on breast cancer. Understanding this mediating pathway is crucial since simply advocating for weight gain in childhood is clearly not a desirable goal. This finding is exciting because showing that adult MD is modifiable during the pubertal growth period means there could be opportunities to intervene during adolescence to reduce lifetime MD and associated breast cancer risk [18]. Further understanding of the underlying mechanism and biological pathways is required to explore potential avenues for intervention. In the study, we also showed that the density-increasing effect of later menarche may be due to lower adiposity in adolescence, which is associated with later puberty rather than an effect of age at menarche directly. The mechanisms linking childhood body size and age at menarche to breast cancer risk could therefore be entirely different and acting in opposing directions. Lastly, we found that genetic instruments for MD are heterogenous and pleiotropic, and there are likely several pathways underlying the role of mammographic density in influencing breast cancer risk. As MD GWAS sample sizes increase, this relationship can be further investigated, enhancing our understanding of the genetic basis of MD and its role in the aetiology of breast cancer.

Methods

Data sources

The mammographic density GWAS data used in this study is a meta-analysis of two studies (Hologic study, N=20,311 and GE study, N=3881; in total N=24,192) of non-Hispanic white women aged between 40-74 years from a larger population-based study, RPGEH (Research Program on Genes, Environment and Health), administered by Kaiser Permanente Northern California (KPNC) Division of Research [65], [66]. The cohort details and study design have been described previously in the original publication of this data [32]. Genotypes were re-imputed with an expanded reference panel, including the Haplotype Reference Consortium in addition to the 1000 Genomes Project Phase III data, to improve accuracy for less common variants. The GWAS analyses were adjusted for age at mammogram, BMI, genotype reagent kit, and the first ten principal components of ancestry as described previously [32]. Three mammographic density phenotypes were analysed: dense area (DA), non-dense area (NDA), and percent density (PD). The original MD GWAS published by Sieh *et al* in 2020 [32] was adjusted for BMI. For this study, the GWAS was rerun without this adjustment ("unadjusted GWAS") on a slightly smaller subset of 24,158 women from the original cohort.

Childhood body size, adult body size, and age at menarche data used in this study were obtained from UK Biobank [67]. UK Biobank is a population-based health research resource consisting of approximately 500,000 people, aged between 40–69 years, who were recruited between the years 2006 and 2010 from across the UK. The study design, participants and quality control (QC) methods have been described in detail previously [67]. The GWAS of childhood body size and adult body size used in this study were performed by Richardson *et al* [5] on UK Biobank data (N= 246,511; female-only data). Childhood body size is a categorical trait describing body size at age 10, with three categories ('thinner than average', 'about average', 'plumper than average'), from a questionnaire completed by adult participants of UK Biobank. Adult body size measure was converted from continuous adult BMI in UK biobank into three groups based on the proportions of childhood body size data to ensure that the GWAS results of both measures are comparable [5]. The genetic scores for childhood and adult body size were independently validated in three separate cohorts (the HUNT study (Norway) [68], Young Finns Study [69], and ALSPAC (UK) [5]), which confirmed that the genetic instruments extracted by Richardson *et al* [5] can reliably separate childhood and adult body size as distinct exposures, in addition to being robust to differential measurement error in simulations performed in the original study. Age at menarche GWAS summary data (N=143,819) was accessed through OpenGWAS [70] (gwas.mrcieu.ac.uk) under ID *ukb-b-3768*.

The breast cancer data used in the study is from the Breast Cancer Association Consortium (BCAC) cohort of 2017 (N=228,951; overall sample and ER+/ER- samples, assessed from OpenGWAS under IDs: *ieu-a-1126, ieu-a-1127, ieu-a-1128*) [35] and the latest release of BCAC in 2020 (N=247,173; overall sample and five molecular subtypes: Luminal A, Luminal B1, Luminal B2, HER2-enriched, and triple-negative breast cancer) [71] (details in Supplementary Table S1). The cohort design and genotyping protocol details are described elsewhere (bcac.ccge.medschl.cam.ac.uk/bcac-groups/study-groups/, bcac.ccge.medschl.cam.ac.uk/bcacdata/). The study groups in the BCAC cohort do not include UK Biobank or MD GWAS cohorts. The overall sample results presented throughout the paper are for BCAC 2017 data. The results for BCAC 2020 overall sample are available in all relevant Supplementary tables, and are not shown here due to their similarity.

Mendelian randomization

Mendelian randomization (MR) is an application of instrumental variable analysis where genetic variants are used as instruments to estimate the causal relationship between a modifiable health exposure and a disease outcome [8] [9]. There are three core assumptions that genetic variants need to satisfy to qualify as valid instruments for the causal inference: (1) variants have to be reliably associated with exposure of interest, (2) there cannot be any confounders of the instrument and the

outcome, and (3) variants cannot be independently associated with the outcome, via pathway other than through the exposure (i.e. horizontal pleiotropy) [72].

The analyses in this work were performed using the two-sample (univariable) MR approach, which relies on using GWAS summary statistics of two non-overlapping samples for exposure and outcome [73]. Two-sample MR analyses were performed using the inverse-variance weighted (IVW) method [74]. Alongside IVW, other complementary MR methods were applied to assess the robustness of the causal estimates and to overcome any potential violations of the MR assumptions (e.g. horizontal pleiotropy) (see **Sensitivity analysis** for further details).

We used the two-step MR framework to assess whether an intermediate trait acts as a causal mediator between the exposure and the outcome of interest [75], [76]. Multivariable Mendelian randomization (MVMR) was used to estimate the independent direct effects of two traits together on the outcome [77] [78]. The genetic variants included in MVMR analysis have to be reliably associated with one or both exposures but not completely overlap (i.e. no perfect collinearity), and have to satisfy the MVMR-extended second and third assumptions of the standard MR analysis [46]. Diagnostic methods and sensitivity tests for the robustness of MVMR estimates [46] [79] are described under **Sensitivity analysis**.

All analyses were conducted using R (v4.2.1). Univariable MR analyses and sensitivity tests were performed using the *TwoSampleMR* R package (v0.5.6) [80], which was also used for accessing GWAS summary data deposited in OpenGWAS [70] (gwas.mrcieu.ac.uk). Multivariable MR was carried out using the *MVMR* R package (version 0.2) [77].

For all exposure traits, the instruments were extracted by selecting SNPs with p-value under the $5x10^{-8}$ threshold and clumping the resulting set of variants with r2 = 0.001 using the default LD (linkage disequilibrium) reference panel in *TwoSampleMR* (1000 Genomes Project, European data only). When extracting instruments from the outcome (breast cancer) GWAS summary statistics, unavailable SNPs were substituted by proxies with a minimum LD r2 = 0.8. The rest of the settings were kept to defaults as per the package version number. The number of instruments used in the analysis for all exposures: childhood body size (115), adult body size (173), age at menarche (190), dense area (21), non-dense area (8), percent density (11).

Sensitivity analysis

In addition to the standard MR analysis (IVW), we used MR-Egger [43] and weighted median [44] MR methods to evaluate the validity of the analysed genetic instruments and to overcome and accommodate potential violations of the core MR assumptions. These complementary methods help to support the causal effects found with IVW, as a single method cannot account for all biological and statistical properties that may impact MR estimates. Also a variety of specialised tests were applied, as recommended in [80].

To assess overall horizontal pleiotropy (violation of assumption 3), the intercept in the MR-Egger regression [43] was evaluated, and the heterogeneity among the genetic variants was quantified using Cochran's Q-statistic [45]. The intercept term in MR-Egger regression is a useful indication of whether directional horizontal pleiotropy is driving the results of an MR analysis, under the assumption that any pleiotropic effects are uncorrelated with the magnitude of the SNP exposure association. When the Egger intercept is close to zero (e.g. < 0.002) and the P-value is large, this can be interpreted as no evidence of a substantial directional (horizontal) pleiotropic effect.

When the Q-statistic for heterogeneity (difference in individual ratio estimates) is high and the corresponding p-value is small, this suggests evidence for heterogeneity and possibly horizontal pleiotropy. A high Q-statistic can also be used as an indicator of one or more variant outliers in the analysis, which may also violate the MR assumptions. In univariable MR, heterogeneity may be indicative of horizontal pleiotropy that does not act through one of the exposures. In MVMR, heterogeneity is quantified by Q_A-statistic (also a further modification of Cochran's Q), and small Q_A indicates a lack of heterogeneity in the per-SNP effects [46].

We derived F-statistics in both univariable and MVMR to evaluate the instrument strength [81] [46], with F > 10 indicating sufficient strength for minimal weak instrument bias in the analysis. We also evaluated the possibility of reverse causation via Steiger filtering and assessed whether each instrument explains more variance (R^2) in the exposure rather than in the outcome [82].

Additional sensitivity and outlier analyses

To explore the excessive heterogeneity and potential pleiotropy identified in the effect of MD on breast cancer, we explored the genetic instruments using several outlier detection methods.

First, we applied MR-PRESSO [37], a method that detects overall pleiotropic bias through outlier detection by assessing each genetic variant's contribution to the overall heterogeneity. This method discards influential outliers from the IVW method and uses a distortion test to evaluate the significance of the distortion between the causal estimate before and after the removal of the outlier variants, providing an outlier-corrected pleiotropy-robust causal estimate as a result. The analysis was run using the *MR-PRESSO* R package (v1.0), using the default parameters.

We also used the approach implemented in *Radial-MR* [39] (R package v1.0) to identify outliers with the most weight in the MR analysis and the largest contribution to Cochran's Q statistic for heterogeneity. The analysis was conducted with a p-value threshold (*alpha* parameter) set to Bonferroni corrected for the number of SNPs tested in the analysis (p < 0.05/number of instruments in the exposure) and using modified second-order weights (*weight* parameter).

Finally, to investigate the presence of clustered heterogeneity and assess the possibility of there being several distinct causal mechanisms by which MD may influence breast cancer risk, we performed clustered Mendelian randomization using *MR-Clust* [38] (R package v0.1.0). MR-Clust is a heterogeneity-based clustering algorithm that extends the typical MR assumption that a risk factor can influence an outcome via a single causal mechanism [83] to a framework that allows one or more mechanisms to be detected. The heterogeneity and outliers in the main MR result may indicate that different genetic variants influence the risk factor in distinct ways, e.g., via distinct biological mechanisms.

MR-Clust assigns variants to *K* clusters, where all variants have similar causal ratio estimates, a "null" cluster (variants with a null effect), and a "junk" cluster (non-null variants that do not fit into any of the K clusters). In our analysis, the clusters were formed of variants that had a great conditional probability of assignment (score > 0.9), keeping the results conservative. Due to the limited number of instruments in MD exposure, we kept all clusters regardless of their size (visualised using the MR-Clust package built-in scatter plot).

The outliers identified by MR-PRESSO and Radial-MR analyses, as well as clusters of SNPs detected by MR-Clust, were displayed using single-SNP forest plots to explore individual SNPs heterogeneity. The single-SNP forest plots show the effect of the exposure on the outcome for each SNP separately (i.e. Wald ratio). The plots also included the IVW MR estimate with the identified outliers excluded, and the invididual estimates for identified clusters.

PheWAS

To further examine the genetic instruments of the MD phenotypes and better understand the potential sources of effect heterogeneity, we performed a phenome-wide association study (PheWAS) analysis [40]. We used PhenoScanner V2 (*phenoscanner* R package v1.0) [84] [85] and OpenGWAS database (gwas.mrcieu.ac.uk/phewas/, accessed via *ieugwasr* R package v0.1.5) [70] to query publicly available GWAS data for associations with the SNPs from the MD phenotypes. The query was restricted to European ancestry datasets, retrieving SNP-trait associations of p-value <5e-08.

We presented PheWAS results for each MD SNP grouped by clusters determined by the MR-Clust algorithm. This helped us to review the association differences between clusters of SNPs with the traits identified in GWAS databases, which might explain some of the observed heterogeneity in the MR results.

Gene and pathway exploration

To explore the functional relevance of the identified clusters of MD instruments, we mapped instrument SNPs of each MD phenotype to genes and identified the pathways thay are involved in. For gene mapping we used the SNP2Gene function of FUMA (the Functional Mapping and Annotation of GWAS) platform [86], where we used a 500-kb positional map, and included genes whose expression was associated with the locus in GTEx v8 (breast or adipose tissues). We extracted pathways using the *enrichR* R package (v3.1) [87] (including pathway definitions from Reactome, KEGG, GO terms, and WikiPathway databases). We also used the *ReactomeContentService4R* R package (v1.4.0) [88] to obtain more recent Reactome data (Reactome data in enrichR is only up until 2016). The pathway data was collected for a broader context only, and no formal gene-set overrepresentation analysis was performed.

Mediation analysis

Mediation analysis is used to quantify the effects of an exposure on an outcome, which act directly or indirectly via an intermediate variable (i.e., mediator) [89]. Identifying mediators of the relationship between the exposure and the outcome enables intervention on those mediators to mitigate or strengthen the effects of the exposure [34].

The total effect of exposure on outcome includes both a direct effect and any indirect effects via one or more mediators. The total effect is captured by a standard univariable MR analysis. To decompose direct and indirect effects, we used the results from two-step MR and MVMR in two mediation analysis methods: Difference method and Product method.

For the Difference method, to estimate the indirect effect, we subtracted the direct effect of exposure on the outcome from MVMR (in analysis with the mediator) from the total effect of exposure on the outcome (univariable MR) [55]. In Product method (also known as 'product of coefficients'), the results from two steps of two-step MR analysis (i.e., the effect of exposure on the mediator and the effect of the mediator on the outcome) are multiplied to get the indirect effect [90], [75]. Here, we used the direct effect of the mediator on the outcome from MVMR as the second term in the calculation [89]. To estimate the standard error (SE) and later confidence intervals (CIs) of the indirect effect, we used 'Propagation of errors' approach for the Difference method estimate (as outlined in [55]) and Delta method (also known as Sobel test [91]) for the Product method estimate. Further details on performing mediation analysis are available in the Supplementary materials of our previous work [10]). The mediation analysis calculations are presented in **Supplementary Note 2**.

Code availability

All analyses in this study are available at: https://github.com/mvab/mammographic_density_mr

Data availability

The GWAS data for BCAC 2017 breast cancer (*ieu-a-1126, ieu-a-1127, ieu-a-1128*) and age at menarche (*ukb-b-3768*) was accessed from OpenGWAS (https://gwas.mrcieu.ac.uk). The BCAC 2020 molecular subtype data is available at https://bcac.ccge.medschl.cam.ac.uk/bcacdata/oncoarray/oncoarray-and-combined-summary-result/. Childhood and adult body size GWAS data was published in ref [5].

This study uses data from a GWAS of mammographic density (ref [32]). The RPGEH genotype data are available upon application to the KP Research Bank (https://researchbank.kaiserpermanente.org/). Additional relevant information is available from the authors upon reasonable request.

Funding acknowledgements

M.V. is supported by the University of Bristol Alumni Fund (Professor Sir Eric Thomas Scholarship). B.L.L. is supported by the University of Bristol Vice-Chancellor's fellowship, Academy of Medical Sciences, Elizabeth Blackwell Institute for Health Research (University of Bristol) and the Wellcome Trust Institutional Strategic Support Fund (ISSF3 (204813/Z/16/Z) and AMS (SBF003/1170)). M.V., G.D.S., E.S., T.G.R., R.C.R. work in the UK Medical Research Council Integrative Epidemiology Unit at the University of Bristol supported by Medical Research Council (MC_UU_00032/01, MC_UU_00032/03, MC_UU_00032/04). This work is also supported by a Cancer Research UK programme grant (the Integrative Cancer Epidemiology Programme) (C18281/A29019). W.S., L.A.H., J.H.R., S.E.A are supported by the U.S. National Institutes of Health (R01CA237541, R01CA264987, R01CA166827).

Authors' contributions

M.V., B.L.L., R.C.R., G.D.S., T.G.R., E.S. conceived and designed the study. M.V. performed the analyses, interpreted the results, and wrote the initial draft of the manuscript as well as subsequent drafts with critical input on results interpretation and manuscript revisions from E.S., B.L.L., T.G.R., G.D.S., R.C.R., W.S., L.A.H., J.H.R., S.E.A. Access to mammographic density data was provided by W.S., L.A.H., J.H.R., S.E.A.; J.H.R. performed genome-wide association studies of mammographic density phenotypes unadjusted for BMI.

The corresponding author attests that all listed authors meet authorship criteria and that no others meeting the criteria have been omitted. All authors read and approved the final manuscript.

We would also like to acknowledge Tom Gaunt and Tim Robinson for thoughtful project discussions.

Competing interests

T.G.R. is employed by GSK outside of this work, for unrelated research. All other authors declare no competing interests.

References

[1] H. Sung *et al.*, "Global cancer statistics 2020: GLOBOCAN estimates of incidence and mortality worldwide for 36 cancers in 185 countries," *CA. Cancer J. Clin.*, vol. 0, no. 0, pp. 1–41, 2021.

[2] K. L. Britt, J. Cuzick, and K. A. Phillips, "Key steps for effective breast cancer prevention," *Nature Reviews Cancer*, vol. 20, no. 8. Nature Publishing Group, pp. 417–436, 11-Jun-2020.

[3] H. J. Baer, S. S. Tworoger, S. E. Hankinson, and W. C. Willett, "Body fatness at young ages and risk of breast cancer throughout life," *Am. J. Epidemiol.*, vol. 171, no. 11, pp. 1183–1194, 2010.

[4] A. Furer *et al.*, "Adolescent obesity and midlife cancer risk: a population-based cohort study of 2·3 million adolescents in Israel," *Lancet Diabetes Endocrinol.*, vol. 8, no. 3, pp. 216–225, 2020.

[5] T. G. Richardson, E. Sanderson, B. Elsworth, K. Tilling, and G. Davey Smith, "Use of genetic variation to separate the effects of early and later life adiposity on disease risk: Mendelian randomisation study," *BMJ*, vol. 369, 2020.

[6] B. W. Jensen *et al.*, "Childhood body mass index trajectories, adult-onset type 2 diabetes, and obesity-related cancers," *J. Natl. Cancer Inst.*, vol. 115, no. 1, pp. 43–51, Jan. 2023.

[7] Y. Hao *et al.*, "Reassessing the causal role of obesity in breast cancer susceptibility – a comprehensive multivariable Mendelian randomization investigating the distribution and timing of exposure," *Int. J. Epidemiol.*, vol. 52, no. 1, p. 58, Jul. 2022.

[8] S. Ebrahim and G. Davey Smith, "Mendelian randomization: Can genetic epidemiology help redress the failures of observational epidemiology?," *Int. J. Epidemiol.*, vol. 32, no. 1, pp. 1–22, Feb. 2003.

[9] E. Sanderson *et al.*, "Mendelian randomization," *Nat. Rev. Methods Prim.*, vol. 2, no. 1, Dec. 2022.

[10] M. Vabistsevits, G. Davey Smith, E. Sanderson, T. G. Richardson, B. Lloyd-Lewis, and R. C. Richmond, "Deciphering how early life adiposity influences breast cancer risk using Mendelian randomization," *Commun. Biol.*, vol. 5, no. 1, 2022.

[11] N. F. Boyd *et al.*, "Heritable dense breasts & breast cancer," vol. 6, no. October, pp. 798–808, 2005.

[12] A. Pettersson *et al.*, "Mammographic density phenotypes and risk of breast cancer: a meta-analysis," *J. Natl. Cancer Inst.*, vol. 106, no. 5, May 2014.

[13] K. A. Bertrand *et al.*, "Dense and nondense Mammographic area and risk of breast cancer by age and tumor characteristics," *Cancer Epidemiol. Biomarkers Prev.*, vol. 24, no. 5, pp. 798–809, May 2015.

[14] V. A. McCormack and I. Dos Santos Silva, "Breast density and parenchymal patterns as markers of breast cancer risk: A meta-analysis," *Cancer Epidemiol. Biomarkers Prev.*, vol. 15, no. 6, pp. 1159–1169, Jun. 2006.

[15] J. Stone *et al.*, "The heritability of mammographically dense and nondense breast tissue," *Cancer Epidemiol. Biomarkers Prev.*, vol. 15, no. 4, pp. 612–617, Apr. 2006.

[16] G. Kleinstern *et al.*, "Association of mammographic density measures and breast cancer 'intrinsic' molecular subtypes," vol. 187, pp. 215–224, 2021.

[17] M. S. Shawky, C. W. Huo, M. A. Henderson, A. Redfern, K. Britt, and E. W. Thompson, "A review of the influence of mammographic density on breast cancer clinical and pathological phenotype," *Breast Cancer Res. Treat. 2019 1772*, vol. 177, no. 2, pp. 251–276, Jun. 2019.

[18] A. G. Ghadge, P. Dasari, J. Stone, E. W. Thompson, R. L. Robker, and W. V. Ingman, "Pubertal mammary gland development is a key determinant of adult mammographic density," *Semin. Cell Dev. Biol.*, vol. 114, no. July, pp. 143–158, 2021.

[19] S. X. Sun *et al.*, "Breast physiology: Normal and abnormal development and function," in *The Breast: Comprehensive Management of Benign and Malignant Diseases*, Elsevier, 2017, pp. 37-56.e6.

[20] S. E. Alexeeff *et al.*, "Age at menarche and late adolescent adiposity associated with mammographic density on processed digital mammograms in 24,840 women," *Cancer Epidemiol. Biomarkers Prev.*, vol. 26, no. 9, pp. 1450–1458, Sep. 2017.

[21] S. V. Ward *et al.*, "The association of age at menarche and adult height with mammographic density in the International Consortium of Mammographic Density," *Breast Cancer Res.*, vol. 24, no. 1, pp. 1–16, Dec. 2022.

[22] Collaborative Group on Hormonal Factors in Breast Cancer, "Menarche, menopause, and breast cancer risk: Individual participant meta-analysis, including 118 964 women with breast

cancer from 117 epidemiological studies," *Lancet Oncol.*, vol. 13, no. 11, pp. 1141–1151, 2012.

[23] G. V. Dall and K. L. Britt, "Estrogen Effects on the Mammary Gland in Early and Late Life and Breast Cancer Risk," *Front. Oncol.*, vol. 7, no. MAY, p. 1, May 2017.

[24] N. Brown *et al.*, "The relationship between breast size and anthropometric characteristics," *Am. J. Hum. Biol.*, vol. 24, no. 2, pp. 158–164, Mar. 2012.

[25] M. B. Terry *et al.*, "Do Birth Weight and Weight Gain during Infancy and Early Childhood Explain Variation in Mammographic Density in Women in Midlife? Results from Cohort and Sibling Analyses," *Am. J. Epidemiol.*, vol. 188, no. 2, pp. 294–304, 2019.

[26] F. Juul, V. W. Chang, P. Brar, and N. Parekh, "Birth weight, early life weight gain and age at menarche: a systematic review of longitudinal studies," *Obes. Rev.*, vol. 18, no. 11, pp. 1272–1288, 2017.

[27] C. Prince, L. D. Howe, G. C. Sharp, A. Fraser, and R. C. Richmond, "Establishing the relationships between adiposity and reproductive factors: a multivariable Mendelian randomization analysis," *medRxiv*, p. 2023.03.03.23286615, Mar. 2023.

[28] Z. J. Andersen, J. L. Baker, K. Bihrmann, I. Vejborg, T. I. A. Sørensen, and E. Lynge, "Birth weight, childhood body mass index, and height in relation to mammographic density and breast cancer: A register-based cohort study," *Breast Cancer Res.*, vol. 16, no. 1, pp. 1–11, Jan. 2014.

[29] J. L. Hopper *et al.*, "Childhood body mass index and adult mammographic density measures that predict breast cancer risk," *Breast Cancer Res. Treat.*, vol. 156, no. 1, pp. 163–170, 2016.

[30] Y. Han *et al.*, "Adiposity Change Over the Life Course and Mammographic Breast Density in Postmenopausal Women," *Cancer Prev. Res.*, vol. 13, no. 5, pp. 475–482, 2020.

[31] M. S. Rice *et al.*, "Mammographic density and breast cancer risk: A mediation analysis," *Breast Cancer Res.*, vol. 18, no. 1, p. 94, Sep. 2016.

[32] W. Sieh *et al.*, "Identification of 31 loci for mammographic density phenotypes and their associations with breast cancer risk," *Nat. Commun.*, vol. 11, no. 1, Dec. 2020.

[33] F. Chen *et al.*, "Mendelian randomization analyses of 23 known and suspected risk factors and biomarkers for breast cancer overall and by molecular subtypes," *Int. J. Cancer*, Apr. 2022.

[34] E. Sanderson, "Multivariable Mendelian Randomization and Mediation," *Cold Spring Harb. Perspect. Med.*, 2020.

[35] K. Michailidou *et al.*, "Association analysis identifies 65 new breast cancer risk loci," 2017.

[36] H. Zhang *et al.*, "Genome-wide association study identifies 32 novel breast cancer susceptibility loci from overall and subtype-specific analyses," *Nat. Genet.*, vol. 52, no. 6, pp. 572–581, Jun. 2020.

[37] M. Verbanck, C. Y. Chen, B. Neale, and R. Do, "Detection of widespread horizontal pleiotropy in causal relationships inferred from Mendelian randomization between complex traits and diseases," *Nat. Genet. 2018 505*, vol. 50, no. 5, pp. 693–698, Apr. 2018.

[38] C. N. Foley, A. M. Mason, P. D. W. Kirk, and S. Burgess, "MR-Clust: Clustering of genetic variants in Mendelian randomization with similar causal estimates," *Bioinformatics*, vol. 37, no. 4, pp. 531–541, 2021.

[39] J. Bowden *et al.*, "Improving the visualization, interpretation and analysis of two-sample summary data Mendelian randomization via the Radial plot and Radial regression," *Int. J. Epidemiol.*, vol. 47, no. 4, pp. 1264–1278, Aug. 2018.

[40] L. A. C. Millard, N. M. Davies, N. J. Timpson, K. Tilling, P. A. Flach, and G. Davey Smith, "MR-PheWAS: Hypothesis prioritization among potential causal effects of body mass index on many outcomes, using Mendelian randomization," *Sci. Rep.*, vol. 5, no. 1, pp. 1–17, Nov. 2015.

[41] V. W. Skrivankova *et al.*, "Strengthening the reporting of observational studies in epidemiology using mendelian randomisation (STROBE-MR): explanation and elaboration," *BMJ*, vol. 375, Oct. 2021.

[42] V. W. Skrivankova *et al.*, "Strengthening the Reporting of Observational Studies in Epidemiology Using Mendelian Randomization: The STROBE-MR Statement," *JAMA*, vol. 326, no. 16, pp. 1614–1621, Oct. 2021.

[43] J. Bowden, G. Davey Smith, and S. Burgess, "Mendelian randomization with invalid instruments: Effect estimation and bias detection through Egger regression," *Int. J. Epidemiol.*, vol. 44, no. 2, pp. 512–525, May 2015.

[44] J. Bowden, G. Davey Smith, P. C. Haycock, and S. Burgess, "Consistent Estimation in Mendelian Randomization with Some Invalid Instruments Using a Weighted Median Estimator," *Genet. Epidemiol.*, vol. 40, no. 4, pp. 304–314, May 2016.

[45] J. Bowden *et al.*, "Improving the accuracy of two-sample summary-data Mendelian randomization: Moving beyond the NOME assumption," *Int. J. Epidemiol.*, vol. 48, no. 3, pp. 728–742, 2019.

[46] E. Sanderson, W. Spiller, and J. Bowden, "Testing and correcting for weak and pleiotropic instruments in two-sample multivariable Mendelian randomization," *Stat. Med.*, vol. 40, no. 25, pp. 5434–5452, Apr. 2021.

[47] J. Yarmolinsky *et al.*, "Causal inference in cancer epidemiology: What is the role of mendelian randomization?," *Cancer Epidemiology Biomarkers and Prevention*, vol. 27, no. 9. American Association for Cancer Research Inc., pp. 995–1010, 01-Sep-2018.

[48] S. Lindström *et al.*, "Genome-wide association study identifies multiple loci associated with both mammographic density and breast cancer risk," *Nat. Commun.*, vol. 5, p. 5303, Oct. 2014.

[49] P. Fernandez-Navarro *et al.*, "Genome wide association study identifies a novel putative mammographic density locus at 1q12-q21," *Int. J. Cancer*, vol. 136, no. 10, pp. 2427–2436, May 2015.

[50] N. Eriksson *et al.*, "Genetic variants associated with breast size also influence breast cancer risk," *BMC Med. Genet.*, vol. 13, Jun. 2012.

[51] M. J. Sherratt, J. C. McConnell, and C. H. Streuli, "Raised mammographic density: Causative mechanisms and biological consequences," *Breast Cancer Res.*, vol. 18, no. 1, pp. 1–9, May 2016.

[52] N. F. Boyd, L. J. Martin, M. J. Yaffe, and S. Minkin, "Mammographic density and breast cancer risk: current understanding and future prospects," *Breast Cancer Res.*, vol. 13, no. 6, Nov. 2011.

[53] F. P. Hartwig, K. Tilling, G. Davey Smith, D. A. Lawlor, and M. C. Borges, "Bias in two-sample Mendelian randomization when using heritable covariable-adjusted summary associations," *Int. J. Epidemiol.*, vol. 50, no. 5, pp. 1639–1650, 2021.

[54] J. Gilbody, M. C. Borges, G. Davey Smith, and E. Sanderson, "Multivariable MR can mitigate bias in two-sample MR using covariable-adjusted summary associations," *medRxiv*, p. 2022.07.19.22277803, Jul. 2022.

[55] S. Burgess, D. J. Thompson, J. M. B. Rees, F. R. Day, J. R. Perry, and K. K. Ong, "Dissecting causal pathways using mendelian randomization with summarized genetic data: Application to age at menarche and risk of breast cancer," *Genetics*, vol. 207, no. 2, pp. 481–487, Oct. 2017.

[56] A. Balmain, "Peto's paradox revisited: black box vs mechanistic approaches to understanding the roles of mutations and promoting factors in cancer," *Eur. J. Epidemiol.*, vol. 1, pp. 1–8, Dec. 2022.

[57] M. Archer, P. Dasari, A. Evdokiou, and W. V. Ingman, "Biological mechanisms and therapeutic opportunities in mammographic density and breast cancer risk," *Cancers (Basel).*, vol. 13, no. 21, pp. 1–21, 2021.

[58] W. Wang *et al.*, "Clustered Mendelian randomization analyses identify distinct and opposing pathways in the association between genetically influenced insulin-like growth factor-1 and type 2 diabetes mellitus," *Int. J. Epidemiol.*, vol. 51, no. 6, pp. 1874–1885, Jun. 2022.

[59] J. S. Brand, K. Humphreys, J. Li, R. Karlsson, P. Hall, and K. Czene, "Common genetic variation and novel loci associated with volumetric mammographic density," *Breast Cancer Res.*, vol. 20, no. 1, Apr. 2018.

[60] A. Khorshid Shamshiri, M. Alidoust, M. Hemmati Nokandei, A. Pasdar, and F. Afzaljavan, "Genetic architecture of mammographic density as a risk factor for breast cancer: a systematic review," *Clin. Transl. Oncol. 2023*, pp. 1–19, Jan. 2023.

[61] H. Chen *et al.*, "Genome-wide and transcriptome-wide association studies of mammographic density phenotypes reveal novel loci," *Daniel S. McConnell*, vol. 21, no. 1, p. 27, Dec. 2022.

[62] Y. Liu *et al.*, "A genome-wide association study of mammographic texture variation," *Breast Cancer Res. 2022 241*, vol. 24, no. 1, pp. 1–15, Nov. 2022.

[63] E. T. Warner *et al.*, "Automated percent mammographic density, mammographic texture variation, and risk of breast cancer: a nested case-control study," *NPJ breast cancer*, vol. 7, no. 1, Dec. 2021.

[64] A. Burkholder *et al.*, "Investigation of the adolescent female breast transcriptome and the impact of obesity," *Breast Cancer Res.*, vol. 22, no. 1, pp. 1–14, 2020.

[65] Y. Banda *et al.*, "Characterizing race/ethnicity and genetic ancestry for 100,000 subjects in the genetic epidemiology research on adult health and aging (GERA) cohort," *Genetics*, vol. 200, no. 4, pp. 1285–1295, Aug. 2015.

[66] M. N. Kvale *et al.*, "Genotyping informatics and quality control for 100,000 subjects in the

genetic epidemiology research on adult health and aging (GERA) cohort," *Genetics*, vol. 200, no. 4, pp. 1051–1060, Aug. 2015.

[67] C. Sudlow *et al.*, "UK Biobank: An Open Access Resource for Identifying the Causes of a Wide Range of Complex Diseases of Middle and Old Age," *PLoS Med.*, vol. 12, no. 3, Mar. 2015.

[68] M. Brandkvist *et al.*, "Separating the genetics of childhood and adult obesity: a validation study of genetic scores for body mass index in adolescence and adulthood in the HUNT Study," *Hum. Mol. Genet.*, vol. 29, no. 24, pp. 3966–3973, Dec. 2020.

[69] T. G. Richardson *et al.*, "Evaluating the direct effects of childhood adiposity on adult systemic metabolism: a multivariable Mendelian randomization analysis," *Int. J. Epidemiol.*, Mar. 2021.

[70] B. Elsworth *et al.*, *The MRC IEU OpenGWAS data infrastructure*. 2020, p. 2020.08.10.244293.

[71] H. Zhang *et al.*, "Genome-wide association study identifies 32 novel breast cancer susceptibility loci from overall and subtype-specific analyses," *Nat. Genet.*

[72] D. A. Lawlor, R. M. Harbord, J. A. C. Sterne, N. Timpson, and G. Davey Smith, "Mendelian randomization: Using genes as instruments for making causal inferences in epidemiology," *Stat. Med.*, vol. 27, no. 8, pp. 1133–1163, Apr. 2008.

[73] S. Burgess, R. A. Scott, N. J. Timpson, G. Davey Smith, and S. G. Thompson, "Using published data in Mendelian randomization: A blueprint for efficient identification of causal risk factors," *Eur. J. Epidemiol.*, vol. 30, no. 7, pp. 543–552, Jul. 2015.

[74] S. Burgess, A. Butterworth, and S. G. Thompson, "Mendelian randomization analysis with multiple genetic variants using summarized data," *Genet. Epidemiol.*, vol. 37, no. 7, pp. 658–665, Nov. 2013.

[75] C. L. Relton and G. Davey Smith, "Two-step epigenetic mendelian randomization: A strategy for establishing the causal role of epigenetic processes in pathways to disease," *Int. J. Epidemiol.*, vol. 41, no. 1, pp. 161–176, 2012.

[76] J. Zheng *et al.*, "Recent Developments in Mendelian Randomization Studies," *Curr. Epidemiol. Reports*, vol. 4, no. 4, pp. 330–345, 2017.

[77] E. Sanderson, G. Davey Smith, F. Windmeijer, and J. Bowden, "An examination of multivariable Mendelian randomization in the single-sample and two-sample summary data settings," *Int. J. Epidemiol.*, vol. 48, no. 3, pp. 713–727, Jun. 2019.

[78] S. Burgess and S. G. Thompson, "Multivariable Mendelian randomization: The use of pleiotropic genetic variants to estimate causal effects," *Am. J. Epidemiol.*, vol. 181, no. 4, pp. 251–260, 2015.

[79] J. M. B. Rees, A. M. Wood, and S. Burgess, "Extending the MR-Egger method for multivariable Mendelian randomization to correct for both measured and unmeasured pleiotropy," *Stat. Med.*, vol. 36, no. 29, pp. 4705–4718, Dec. 2017.

[80] G. Hemani *et al.*, "The MR-base platform supports systematic causal inference across the human phenome," *Elife*, vol. 7, May 2018.

[81] S. Burgess and S. G. Thompson, "Avoiding bias from weak instruments in Mendelian randomization studies," *Int. J. Epidemiol.*, vol. 40, no. 3, pp. 755–764, Jun. 2011.

[82] G. Hemani, K. Tilling, and G. Davey Smith, "Orienting the causal relationship between imprecisely measured traits using GWAS summary data," *PLoS Genet.*, vol. 13, no. 11, pp. 1–22, 2017.

[83] S. Burgess, C. N. Foley, and V. Zuber, "Inferring causal relationships between risk factors and outcomes using genetic variation," *Handb. Stat. Genomics*, vol. 1, pp. 651–677, 2019.

[84] M. A. Kamat *et al.*, "PhenoScanner V2: an expanded tool for searching human genotype-phenotype associations," *Bioinformatics*, vol. 35, no. 22, pp. 4851–4853, Nov. 2019.

[85] J. R. Staley *et al.*, "PhenoScanner: a database of human genotype-phenotype associations," *Bioinformatics*, vol. 32, no. 20, pp. 3207–3209, Oct. 2016.

[86] K. Watanabe, E. Taskesen, A. Van Bochoven, and D. Posthuma, "Functional mapping and annotation of genetic associations with FUMA," *Nat. Commun.*, vol. 8, no. 1, Dec. 2017.

[87] M. V. Kuleshov *et al.*, "Enrichr: a comprehensive gene set enrichment analysis web server 2016 update," *Nucleic Acids Res.*, vol. 44, no. W1, pp. W90–W97, 2016.

[88] C.-L. Poon, "ReactomeContentService4R: Interface for the Reactome Content Service [R package]." 2022.

[89] A. R. Carter *et al.*, "Mendelian randomisation for mediation analysis: Current methods and challenges for implementation," *European Journal of Epidemiology*. 2021.

[90] S. Burgess, R. M. Daniel, A. S. Butterworth, and S. G. Thompson, "Network Mendelian randomization: Using genetic variants as instrumental variables to investigate mediation in causal pathways," *Int. J. Epidemiol.*, vol. 44, no. 2, pp. 484–495, 2015.

[91] M. E. Sobel, "Asymptotic Confidence Intervals for Indirect Effects in Structural Equation

Models," *Sociol. Methodol.*, vol. 13, pp. 290–312, 1982.